EJN European Journal of Neuroscience

FENS Federation of European Neuroscience Societies

European Journal of Neuroscience, Vol. 41, pp. 157–167, 2015 doi:10.1111/ejn.12779

NEUROSYSTEMS

Distinct subsynaptic localization of type 1 metabotropic glutamate receptors at glutamatergic and GABAergic synapses in the rodent cerebellar cortex

Mahnaz Mansouri,[1,*] Yu Kasugai,[1,*] Yugo Fukazawa,[2] Federica Bertaso,[3,4,5] Fabrice Raynaud,[3,4,5] Julie Perroy,[3,4,5] Laurent Fagni,[3,4,5] Walter A. Kaufmann,[1] Masahiko Watanabe,[6] Ryuichi Shigemoto[2] and Francesco Ferraguti[1]

[1]Department of Pharmacology, Innsbruck Medical University, Innsbruck, Austria
[2]Division of Cerebral Structure, National Institute for Physiological Sciences, Okazaki, Japan
[3]CNRS, UMR-5203, Institut de Génomique Fonctionnelle, Montpellier, France
[4]INSERM, U661, Montpellier, France
[5]Universités de Montpellier 1 & 2, UMR-5203, Montpellier, France
[6]Department of Anatomy, Hokkaido University, Sapporo, Japan

Keywords: freeze-fracture, Homer, parallel fibres, Purkinje cell

Abstract

Type 1 metabotropic glutamate (mGlu1) receptors play a pivotal role in different forms of synaptic plasticity in the cerebellar cortex, e.g. long-term depression at glutamatergic synapses and rebound potentiation at GABAergic synapses. These various forms of plasticity might depend on the subsynaptic arrangement of the receptor in Purkinje cells that can be regulated by protein–protein interactions. This study investigated, by means of the freeze-fracture replica immunogold labelling method, the subcellular localization of mGlu1 receptors in the rodent cerebellum and whether Homer proteins regulate their subsynaptic distribution. We observed a widespread extrasynaptic localization of mGlu1 receptors and confirmed their peri-synaptic enrichment at glutamatergic synapses. Conversely, we detected mGlu1 receptors within the main body of GABAergic synapses onto Purkinje cell dendrites. Although Homer proteins are known to interact with the mGlu1 receptor C-terminus, we could not detect Homer3, the most abundant Homer protein in the cerebellar cortex, at GABAergic synapses by pre-embedding and post-embedding immunoelectron microscopy. We then hypothesized a critical role for Homer proteins in the peri-junctional localization of mGlu1 receptors at glutamatergic synapses. To disrupt Homer-associated protein complexes, mice were tail-vein injected with the membrane-permeable dominant-negative TAT-Homer1a. Freeze-fracture replica immunogold labelling analysis showed no significant alteration in the mGlu1 receptor distribution pattern at parallel fibre–Purkinje cell synapses, suggesting that other scaffolding proteins are involved in the peri-synaptic confinement. The identification of interactors that regulate the subsynaptic localization of the mGlu1 receptor at neurochemically distinct synapses may offer new insight into its trafficking and intracellular signalling.

Introduction

The cerebellum plays a key role in the coordination of movements as well as in the regulation of sensory, emotional and cognitive functions (Ito, 2001, 2006). Recent evidence suggests that multiple forms of plasticity regulate the acquisition, dynamics and consolidation of these learned behaviours (Boyden *et al.*, 2004; Wang *et al.*, 2014). The computations required to accomplish these different forms of plasticity occur in the topographically organized excitatory and inhibitory inputs to dendritic spines and shafts, respectively, of Purkinje cells (PCs), the sole output neurons of the cerebellar cortex, which are in turn controlled by several distinct interneurons (Raymond *et al.*, 1996).

The PCs abundantly express in their spines and dendrites the type 1 metabotropic glutamate (mGlu1) receptor, which exists as multiple splice variants (Ferraguti *et al.*, 2008). All mGlu1 isoforms are expressed by PCs including mGlu1α (Ferraguti *et al.*, 2008), which possesses the longest C-terminus tail, enabling it to directly interact with multiple intracellular partners such as the Homer family of scaffolding proteins (Xiao *et al.*, 2000). In PCs, mGlu1 receptors critically contribute to synaptic long-term depression after synchronous and repeated firing of parallel fibres (PFs) and climbing fibres (Aiba *et al.*, 1994; Conquet *et al.*, 1994; Shigemoto *et al.*, 1994; Dzubay & Otis, 2002). In addition to long-term depression, mGlu1 receptors have been implicated in a number of other important activity-dependent synaptic changes at PC glutamatergic synapses, such as depolarization-induced suppression of excitation (Maejima *et al.*, 2001). Plastic changes also occurring at GABAergic synapses were

Correspondence: Francesco Ferraguti, as above.
E-mail: francesco.ferraguti@i-med.ac.at

*M.M. and Y.K. contributed equally to this work.

Received 7 April 2014, revised 26 September 2014, accepted 5 October 2014

shown to depend on mGlu1 receptors. These include depolarization-induced suppression of inhibition (DSI) (Galante & Diana, 2004) and rebound potentiation (RP) (Sugiyama *et al.*, 2008).

The way in which mGlu1 receptors influence these various forms of plasticity probably arises from their precise localization and arrangement at synapses, as well as from their interaction with different scaffolding and signalling proteins (Ferraguti *et al.*, 2008). Post-embedding immunogold labelling showed a peri-synaptic accumulation of mGlu1 receptors in an annulus surrounding the post-synaptic density (PSD) of both types of PF–PC and climbing fibre–PC excitatory inputs (Baude *et al.*, 1993; Nusser *et al.*, 1994; Lujan *et al.*, 1997; Mateos *et al.*, 2000), indicating a direct participation in the molecular plasticity mechanisms at these synapses (Kano *et al.*, 2008). However, a spatial association between mGlu1 receptors and GABAergic synapses in the cerebellar cortex remains unexplored. Previous work in the basal ganglia suggested that mGlu1 receptors could reside in the main body of type II symmetric synapses (Hanson & Smith, 1999). However, because of the limitations of the pre-embedding immunolabelling method for the detection of intrasynaptic proteins, conclusive evidence for the presence of mGlu1 receptors in GABAergic synapses awaits the use of more sensitive approaches. With this aim in mind, we have exploited the freeze-fracture replica immunogold labelling (FRIL) method, which allows the visualization of integral membrane proteins with high spatial resolution and high sensitivity (Masugi-Tokita & Shigemoto, 2007). In addition, to address the mechanisms underlying the characteristic peri-junctional localization of mGlu1 receptors in glutamatergic synapses, we have investigated the role of the long Homer proteins by intravenous injection of the dominant-negative Homer1a fused with the cell-penetrating peptide TAT.

Materials and methods

Ethical standards

Experimental procedures on animals were approved by the Austrian Animal Experimentation Ethics Board (GZ66.011/83-BrGT/2005 and GZ66.011/28-BrGT/2009) and the National Institute for Physiological Science's Animal Care and Use Committee, and were in accordance with directives of the French Ministry of Agriculture, in compliance with both the European Convention for the Protection of Vertebrate Animals used for Experimental and Other Scientific Purposes (ETS no. 123) and the European Communities Council Directive of 24 November 1986 (86/609/EEC). The authors further attest that all efforts were made to minimize the number of animals used, and to use alternatives to *in vivo* techniques whenever available.

Experimental animals

Both adult male rats and mice were used for this study. Sprague Dawley rats (300–400 g) were obtained from the Department of Laboratory Animals and Genetics ($n = 5$; Medical University Vienna, Vienna, Austria) and Japan SLC Inc. ($n = 3$; Hamamatsu, Japan). Adult male C57Bl/6 mice ($n = 11$; 25–30 g; Charles River, Sulzfeld, Germany) as well as mGlu1-knockout (KO) mice ($n = 5$; backcrossed in C57Bl/6 for five generations) and wild-type littermate mice ($n = 5$; bred at the Department of Pharmacology, Innsbruck, Austria) were also used. Injection of TAT-Homer1a or TAT-HomerW24Y was carried out in adult male Swiss mice ($n = 14$; 8 weeks old; Janvier, St Berthevin, France). Before use, the animals were housed in groups of four to five under controlled laboratory conditions (12:12 h light/dark cycle with lights on at 07:00 h; 21 ± 1 °C; 60% humidity) with food and water *ad libitum* for at least 2 weeks after delivery from the supplier. Animals were deeply anesthetized by intraperitoneal injection of thiopental (150 mg/kg, i.p.) and perfused transcardially with phosphate-buffered saline (PBS) (0.9% NaCl, pH 7.4) followed by ice-cold fixative.

Suppliers

Thiopental was obtained from Sandoz (Kundl, Austria). Normal goat serum, biotinylated antibodies and the avidin-biotinylated horseradish peroxidase complex were purchased from Vector Laboratories (Burlingame, USA). Fab fragments and antibodies coupled to nanogold particles as well as the HQ silver enhancement kit were obtained from Nanoprobes (Stony Brook, NY, USA). Paraformaldehyde, osmium tetroxide and uranyl acetate were from Agar Scientific Ltd (Stansted, UK). Electron microscopic grade glutaraldehyde was purchased from Polysciences Inc. (Warrington, PA, USA) and picric acid from Fluka GmbH (Buchs, Switzerland). Dynabeads Protein-A, Seeblue Plus2 Prestained Protein Marker, NuPAGE 4–12% Bis-Tris gel and 3-(N-Morpholino) propanesulfonic acid sodium dodecyl sulfate Running Buffer were all obtained from Invitrogen. The polyvinylidene difluoride membrane and ECL Prime were from GE Healthcare. All other chemicals were purchased from Sigma (Vienna, Austria).

Reagents

The source of the antibodies, antigen used, specificity and dilutions are given in Table 1. Whenever possible, the specificity of primary antibodies was tested in tissue from KO animals. To control for possible cross-reactivity between IgGs in double-immunolabelling experiments, some sections were processed through the same immunocytochemical sequence except that only one primary antibody was applied, but the full complement of secondary antibodies was maintained. All of these control reactions resulted in a lack of labelling of the species-unrelated secondary antibodies, further confirming the specificity of the immunosignals.

Immunocytochemistry for light and pre-embedding electron microscopy

For these experiments animals were perfused with a fixative made of 4% w/v paraformaldehyde and 15% v/v of a saturated solution of picric acid in phosphate buffer (PB) (0.1 M, pH 7.4) for 15 min for rats or 10 min for mice. For electron microscopy experiments glutaraldehyde (25%) at a final dilution of 0.05% v/v was added to the fixative just before the perfusion. Brains were then immediately removed from the skull, washed in 0.1 M PB and sliced coronally in 40-μm-thick (for light microscopy) or 70-μm-thick (for electron microscopy) sections on a vibratome (VT1000S, Leica Microsystems, Vienna, Austria). Sections were stored in 0.1 M PB containing 0.05% sodium azide at 6 °C until use. Pre-embedding immunocytochemistry experiments were carried out according to previously published procedures (Sreepathi & Ferraguti, 2012). Briefly, free-floating sections were freeze–thawed twice after cryoprotection in 20% sucrose in 0.1 M PB to allow antibody penetration, and then incubated in 20% normal goat serum in Tris-buffered saline (TBS) for 2 h at 21 °C–23 °C (room temperature, RT). After blocking, sections were exposed first to primary antibodies (see Table 1) for ~72 h at 6 °C and then with the appropriate secondary antibodies (Table 1) overnight at 6 °C, both made up in a solution containing 2% normal goat serum in TBS. For light microscopy the immunore-

TABLE 1. Concentrations and combinations of primary and secondary antibodies

Primary antibody	Source and specificity	Antigen	Species	Dilution	Secondary antibody	Dilution	Combinations
mGlu1α C-t	Shigemoto *et al.* (1994)	Rat aa 859-1199	Rabbit	1 : 1000	BBI 4049, 10 nm, goat	1 : 30	–
				1 : 500	BBI 4847, 5 nm, goat	1 : 30	A
	Frontier Institute Co. Ltd, code no.: mGluR1a-Gp-Af660-1	Mouse aa 945-1127	Guinea pig	1 : 2000	Aurion, 6 nm, goat	1 : 30	B, C
				1 : 1000	BBI 1157, 5 nm, goat	1 : 30	D
	Frontier Institute Co. Ltd, code no.: mGluR1a-Rb-Af811-1	Mouse aa 945-1127	Rabbit	1 : 300	BBI 4847, 5 nm, goat	1 : 30	G
mGlu1 N-t	Ferraguti *et al.* (1998)	Rat aa 82-520	Rabbit	1 : 50	BBI 6013, BBI 12701, 5 nm, goat	1 : 30	E, F
Pan-AMPA	Frontier Institute Co. Ltd, code no.: PanAMPAR-Gp-Af580-1	Mouse aa 717-754	Guinea pig	1 : 200	BBI 5913, 10 nm, goat	1 : 30	E
Glu-δ2 N-t	Masugi-Tokita & Shigemoto (2007)	Mouse aa 520-533	Guinea pig	1 : 500	BBI 5913, 10 nm, goat	1 : 30	F
					BBI 1175, 5 nm, goat	1 : 30	–
Glu-δ2 C-t	Frontier Institute Co. Ltd, code no.: GluRd2C-Rb-Af500-1	Mouse aa 852-931	Rabbit	1 : 100	BBI 6259, 10 nm, goat	1 : 30	D
					Amersham, 15 nm, goat	1 : 30	B
$GABA_A$- α1	Kaufmann *et al.* (2009)	Mouse aa 328-382, GST fusion protein	Guinea pig	1 : 100	BBI 5913, 10 nm, goat	1 : 30	A
				1 : 200	Aurion, 6 nm, goat	1 : 30	–
	Kasugai *et al.* (2010)	Rat aa 328-382, GST fusion protein	Rat	1 : 70	BBI 3347, 15 nm, goat	1 : 30	C, G
Homer3 (Vesl 3)	Synaptic System, cat. no. 160 303	Rat aa 122-177	Rabbit	0.8 μg/mL	5 and 10 nm gold	1 : 30	Post-embedding
	Shiraishi *et al.* (2004)	Mouse aa 131-358	Rabbit	1 : 3000	Nanogold	1 : 100	Pre-embedding, LM
c-Myc	Sigma, cat. no. M4439	EQKLISEEDL of human oncogene c-myc	Mouse	1 : 1000	Anti-mouse Cy3-conjugated	1 : 1000	Immunohistochemistry

Capital letters indicate combinations of antibodies used for FRIL reactions. aa, aminoacid; BBI, British Biocell International; C-t, carboxy terminus; Glu, glutamate; GST, glutathione S-transferase; LM, light microscopy; N-t, amino terminus.

action was visualized by means of horseradish peroxidase and 3-3′-diaminobenzidine (0.5 mg/mL). The sections were then mounted onto gelatin-coated glass slides, dehydrated (50%, 70%, 90%, 95%, 100% and butylacetate) and finally coverslipped with Eukitt (Agar Scientific Ltd). Analysis was performed under an AxioPhot microscope (Zeiss, Jena, Germany). Images were taken through an AxioCam camera (Zeiss) by means of the OPENLAB software (version 5.5.0; Improvision, Coventry, UK).

For electron microscopy the immunoreaction was visualized by means of a nanogold–silver-enhanced reaction. Sections were incubated overnight with Fab′ fragment secondary antibodies conjugated to nanogold particles (1.4 nm), then extensively washed in milliQ water followed by silver enhancement of the gold particles using the HQ kit (Nanoprobes) for ~10–12 min. After extensive washes in milliQ water and 0.1 M PB, the sections were treated with 2% OsO_4 in 0.1 M PB for 40 min at RT. Contrast was enhanced with 1% uranyl acetate in 50% ethanol for 30 min at RT. Sections were dehydrated by graded ethanol (50%, 70%, 90%, 100%) and propylene oxide at RT, and then quickly transferred into weighing boats containing epoxy resin (Durcupan ACM-Fluka, Sigma) where they were kept overnight at RT. The following day, the sections were transferred onto siliconized slides, coverslipped with ACLAR® film coverslips (Ted Pella, Inc., Redding, CA, USA), and incubated for 3 days at 60 °C. Blocks of the cerebellar cortex were cut under a stereomicroscope and re-embedded in epoxy resin. Ultrathin sections (70 nm) were cut using a diamond knife (Diatome, Switzerland) on an ultramicrotome (Ultracut, Leica), collected on single-slot copper grids coated with pioloform (Agar Scientific Ltd) and analysed in a transmission electron microscope (CM120, Philips, Eindhoven, the Netherlands) equipped with a Morada CCD camera (Soft Imaging Systems, Münster, Germany).

Post-embedding immunogold labelling

For post-embedding experiments animals were perfused with a fixative solution containing 4% paraformaldehyde and 0.05% glutaraldehyde for 15 min, with no post-fixation. Tissue blocks were dissected from the cerebellar cortex, freeze-substituted and embedded at low temperature in Lowicryl HM20 resin. Ultrathin sections (70–80 nm) were cut on an ultramicrotome, mounted on formvar-coated nickel mesh grids, and processed for immunogold cytochemistry as previously described (Kaufmann *et al.*, 2009). Sections were etched with 1% H_2O_2 in TBS for 20 min at RT, followed by incubation in 50 mM glycine in TBS containing 0.1% Triton X-100 (TBS-T) (pH 7.4) for 10 min at RT. After application of 2% bovine serum albumin, 2% normal goat serum and 0.2% milk powder in TBS-T for 20 min to block non-specific binding sites, sections were incubated with primary antibodies (Table 1) diluted in TBS-T containing 2% bovine serum albumin overnight at 7 °C. After rinsing in TBS-T, gold-conjugated goat anti-rabbit secondary antibody was applied (diluted 1 : 30 in TBS-T containing 2% bovine serum albumin and 0.05% polyethylene glycol) for 90 min at RT. The sections were then rinsed in double-distilled water and air-dried. The sections were stained with uranyl acetate (4% uranyl acetate w/v in 50% ethanol; 1.5 min at RT) and 0.3% lead citrate (1.5 min at RT), and examined in a Philips CM120 transmission electron microscope.

TAT-Homer1a expression and purification

A DNA plasmid containing the open reading frame for Homer1a was encoded under the control of the cytomegalovirus promoter in pRK5-Homer1a, as previously described (Perroy *et al.*, 2008). The Homer1a coding sequence was fused to the coding sequence of the TAT-permeant peptide to obtain pET-His-Myc-TAT-Homer1a. To engineer pET-His-Myc-TAT-HomerW24Y, we used primers containing the point mutations coding for W24Y (5′-ACA-AAGAAGAACTATGTACCCACTAGTAAGCAT-3′) to amplify by polymerase chain reaction the Homer1a coding sequence. BL21 (DE3)-competent cells were transformed with either the pET-His-Myc-TAT-Homer1a vector or the pET-His-Myc-TAT-HomerW24Y vector and incubated in lysogeny broth media. Induction of protein synthesis was started by adding isopropyl-beta-D-thiogalactopyranoside (500 μM) for 3 h. His-Myc-TAT-Homer1a protein was purified under denaturing conditions on Ni-nitrilotriacetic acid resin (Qiagen). Cells were lysed in 8 M urea buffer, pH 8, and centrifuged at 10 000 ***g*** for 20 min. Supernatants were loaded on Ni-nitrilotriacetic acid resin and incubated for 60 min to allow for protein binding. The resin was then washed in 8 M urea buffer, pH 6.5. The His-Myc-TAT-Homer1a protein obtained was as follows:

MHHHHHHRPGYGRKKRRQRRRGGLDKLNALSFVDPDEQK LISEEDLGGHMGEQPIFSTRAHVFQIDPNTKKN**W**VPTSKHAVT VSYFYDSTRNVYRIISLDGSKAIINSTITPNMTFTKTSQKFGQWA DSRANTVYGLGFSSEHHLSKFAEKFQEFKEAARLAKEKSQEK MELTSTPSQESAGGDLQSPLTPESINGTDDERTPDVTQNSEPRA EPTQNALPFPHRYTFNSAIMIK. The tryptophan amino acid modified in the W24Y mutant is highlighted in bold and underlined. The poly-His tag and Myc tag are also underlined. His-Myc-TAT-Homer1a was eluted by the addition of 8 M urea buffer, pH 4.5. Just before use, denatured His-Myc-TAT-Homer1a protein was desalted using a PD-10 column (GE Healthcare) and eluted in PBS.

In vivo *TAT-Homer1a protein injection, tissue preparation and immunofluorescence*

Swiss mice were intravenously injected with either a control saline solution (n = 3) or TAT-Homer1a (n = 3; 8 mg/kg each; injection volumes in the caudal vein: 100–150 μL). For immunofluorescence experiments, mice were anaesthetized at 60 min after injection and perfused transcardially with 4% paraformaldehyde in PBS followed by post-fixation for 48 h in the same solution. Brains were cut in sagittal sections (50 μm thick) with a vibratome, permeabilized for 3 h at RT in a solution containing 0.25% Triton, 10% goat and 10% donkey serum in PBS, incubated overnight at 4 °C with mouse anti-Myc antibody (Sigma; 1 : 1000 dilution), rinsed in PBS and incubated for 1 h at RT with an anti-mouse Cy3-conjugated antibody (Jackson Laboratory; 1 : 1000 dilution). Slices were mounted with Mowiol for observation under a Zeiss AxioImager Z1 microscope equipped with Apotome and appropriate epifluorescence and filters (545 ± 25 and 605 ± 70 nm for excitation and emission, respectively). Image quantifications were determined with ImageJ software (National Institutes of Health, USA).

Fracture replica immunogold labelling method

Rats and mice were perfused transcardially for 7 min with a solution containing 0.5% or 1% paraformaldehyde and 15% of a saturated solution of picric acid in 0.1 M PB at a rate of 10 or 5 mL/min, respectively. TAT-Homer1a (n = 3) or TAT-Homer1aW24Y (n = 3)-treated mice were perfused at 30 min after the intravenous injection. Brains were quickly extracted from the skull and sliced (150 μm thickness) on a vibratome (Leica). Slices were cryoprotected in 30% glycerol in 0.1 M PB and high-pressure frozen by means of an HPM 010 machine (Bal-Tec, Balzers, Liechtenstein). The frozen slices were then freeze-fractured at −115 °C and replicated with a first layer of carbon (5 nm), shadowed by platinum (2 nm), and followed by a second carbon layer (15 nm) in a freeze-etching BAF 060 device (Bal-Tec). After thawing, the tissue attached to replicas was solubilized with shaking at 80 °C overnight in the following solubilization solution: 15 mM Tris[hydroxymethyl]-aminomethane, 20% sucrose, and 2.5% sodium dodecyl sulphate, pH 8.3. Immunolabelling of replicas was carried out according to previously published procedures with minor modifications (Kaufmann *et al.*, 2009). Blocking was performed with a solution consisting of 5% bovine serum albumin and 0.1% Tween-20 in TBS (pH 7.4). Replicas were incubated in primary antibodies (Table 1) at 15 °C for

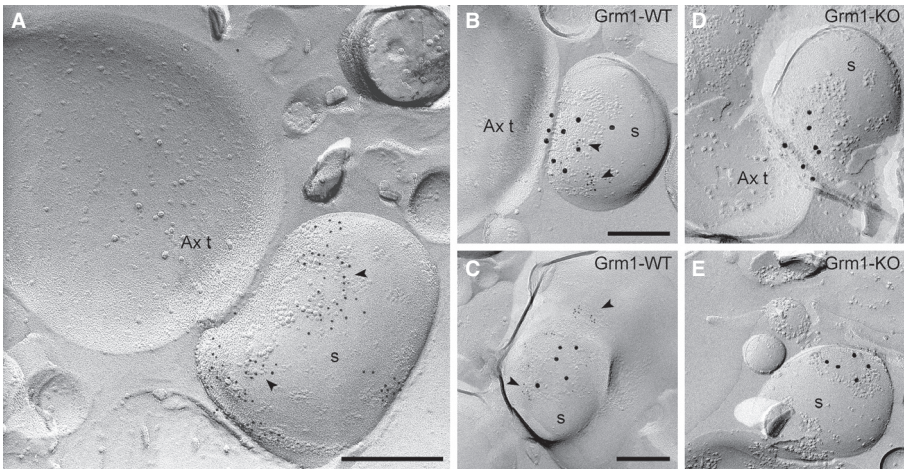

FIG. 1. Peri-synaptic localization of mGlu1α receptors at cerebellar PF–PC synapses. (A) P-face immunogold labelling for mGlu1α receptor (5 nm) at PF–PC synapses in the rat and (B-E) mouse cerebellar cortex as revealed by means of the FRIL method. Immunolabelling was performed with an antibody directed against the C-terminal epitope. A distinct accumulation of gold particles for the mGlu1α receptor (arrowheads) can be observed at the edge of PSDs, confirmed by immunolabelling for Glu-δ2 receptor (15 nm), on PC spines. (D and E) Labelling specificity was confirmed by the absence of labelling for the mGlu1α receptor in replicas made from the cerebella of Grm1-KO mice. Ax t, axon terminal; Grm1-KO, mGlu1-knock out; Grm1-WT, mGlu1-wild type; s, dendritic spine. Scale bars: 230 nm in A; 200 nm in B–D.

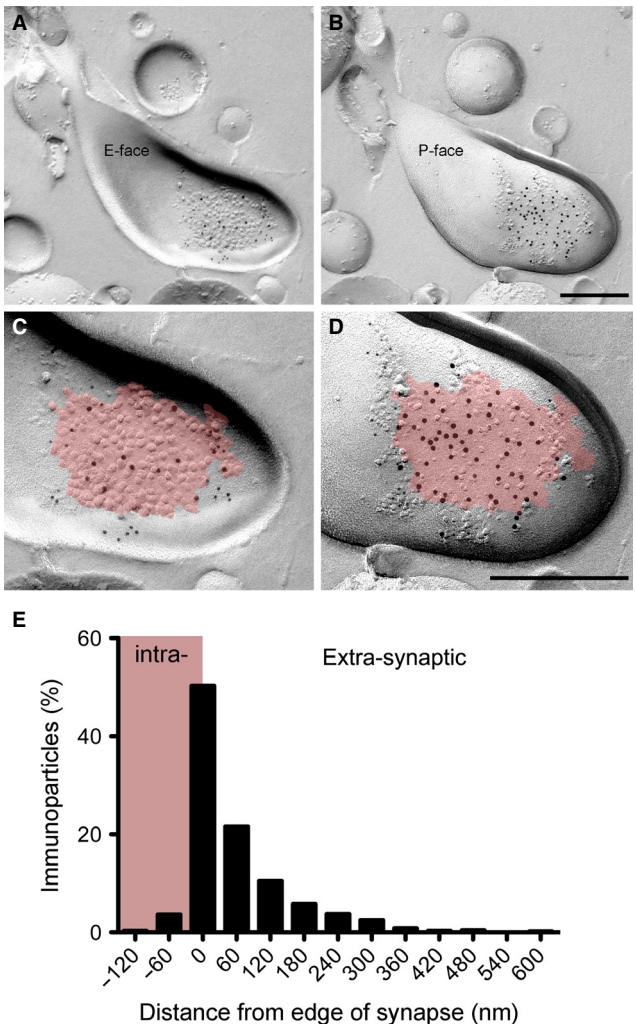

FIG. 2. Plasma membrane leaflet-independent partitioning of mGlu1 receptors and peri-junctional accumulation at rat cerebellar PF–PC synapses. (A and C) Low- and high-magnification micrographs of the exoplasmic face (E-face) of a PC spine double labelled with antibodies directed against the N-terminus of mGlu1 (5 nm) and Glu-δ2 (10 nm) receptors. A typical IMP cluster representing the PSD of the PF–PC synapse is highlighted in pink (C). (B and D) Low- and high-magnification micrographs of the P-face of the same synapse labelled with C-terminal antibodies of mGlu1α (5 nm) and Glu-δ2 (10 nm). In order to reveal the PSD area on the P-face of the spine, the outline on the IMP cluster in the E-face was accurately scaled and replotted onto the P-face membrane (in pink). (E) Frequency distribution of gold particles for the mGlu1 receptor measured from the PSD edge on the E-face of PF–PC synapses in the rat cerebellar cortex. Histograms represent 60-nm-wide bins, as used in previous studies (Lujan *et al.*, 1997; Mateos *et al.*, 2000). The pink area represents the intrasynaptic side. Note the peak in the particle distribution for mGlu1 receptors within the first 60 nm from the PSD edge (number of gold particles analysed = 937; number of animals = 3). Scale bars: 250 nm in A–D.

48 h. Following extensive washes, replicas were incubated with gold-conjugated secondary antibodies, purchased from British Biocell International (Cardiff, UK; 5, 10 and 15 nm), Aurion (Wageningen, Netherland; 6 nm) or Amersham (Buckinghamshire, UK; anti-rabbit, 15 nm), for 2 h at 37 °C. For double-labelling experiments primary and secondary antibodies were incubated in sequence with the antibodies for the detection of mGlu1 always incubated first. The specificity of the antibodies was tested by omitting the primary antibody or by the use of tissue obtained from mGlu1 null mice. For immunostaining with the anti-mGlu1 receptor N-terminal antibody, the solubilization solution was progressively replaced with 5% polyethylene glycol (PEG-6000; Merck, Darmstadt, Germany) in TBS. Replicas were then mounted on pioloform-coated mesh copper grids and examined in a Philips CM120 transmission electron microscope.

Immunoprecipitation and western blotting

Swiss mice were injected intravenously with either TAT-Homer1a (n = 3) or TAT-Homer1aW24Y (n = 3); the cerebella were dissected at 60 min after injection and snap frozen. The cerebella were pooled and homogenized in ice-cold 10 mM Tris-HCl, pH 7.4, buffer containing 320 mM sucrose, 1 mM phenylmethylsulphonyl fluoride, 1 mM NaF, 1 mM Na_3VO_4 and complete EDTA-free protease inhibitors (Roche, Vienna, Austria) using a motorized homogenizer (Sartorius). The P2 fractions were obtained by sequential centrifugation at 1000 ***g*** and 17 000 ***g***. For immunoprecipitation, the detergent lysates were obtained by suspending the P2 fractions in ice-cold 25 mM Tris-HCl, pH 7.5, buffer containing 0.5% sodium deoxycholate, 1% NP-40, 0.1% sodium dodecyl sulfate, 137 mM NaCl, 3 mM KCl, 1 mM phenylmethylsulphonyl fluoride, 1 mM NaF, 1 mM Na_3VO_4 and complete EDTA-free protease inhibitors (Roche) followed by 60 min centrifugation at 20 000 ***g***. Proteins (400 μg) were then incubated with 0.8 μg of mGlu1α receptor polyclonal antibody raised in guinea pig (Frontiers Institute, cat. no. Af660) for 2 h at 6 °C. The antigen–antibody complexes were then incubated with Dynabeads Protein-A (20 μL) and the immunoprecipitation eluates were obtained by heating the samples in Laemmli loading buffer for 10 min at 70 °C. The immunoprecipitation eluates were loaded on a pre-cast Nupage 4–12% Bis-Tris gel (Invitrogen) and then transferred to a polyvinylidene difluoride membrane that was cut below 97 kDa. The upper parts of the polyvinylidene difluoride membranes were immunolabelled with anti-mGlu1α antibodies (1 : 3000, rabbit polyclonal, Frontiers Institute, cat. no. Af811-1). The lower parts of the polyvinylidene difluoride membranes were first immunolabelled with anti-c-Myc antibodies (1 : 5000, mouse monoclonal, Sigma, cat. no. M4439) and, after stripping with β-mercaptoethanol (100 mM), reimmunolabelled with anti-Homer1 (1 : 1000, rabbit polyclonal, Frontiers Institute, cat. no. Af1000-1). Immunoreactive bands were detected by incubating the membranes in horseradish peroxidase-conjugated secondary antibodies (1 : 10 000, Invitrogen) followed by the ECL Prime reagent. Chemiluminescence was visualized with the Fusion SL-4 Vilber Lourmat imaging system (Peqlab, Erlangen, Germany).

Processing of image data

Whole images were contrast-adjusted, sharpened and cropped in Photoshop (Adobe) without changing any specific feature.

Sampling and analysis of gold particles

After immunogold labelling, to establish the distribution of mGlu1 receptors in relation to the synapse, defined as the intramembrane particle (IMP) cluster on the exoplasmic face, we measured the shortest distance from the centre of each 5 nm immunogold particle to the synaptic edge. Values inside the PSD were considered negative and those outside were considered positive. The particles that were present directly on the synaptic edge were given a value equal to zero. A synapse was considered positive for AMPA or Gluδ2 receptors when the PSD contained at least three gold particles. Results were then plotted using Prism-5 for Mac (GraphPad

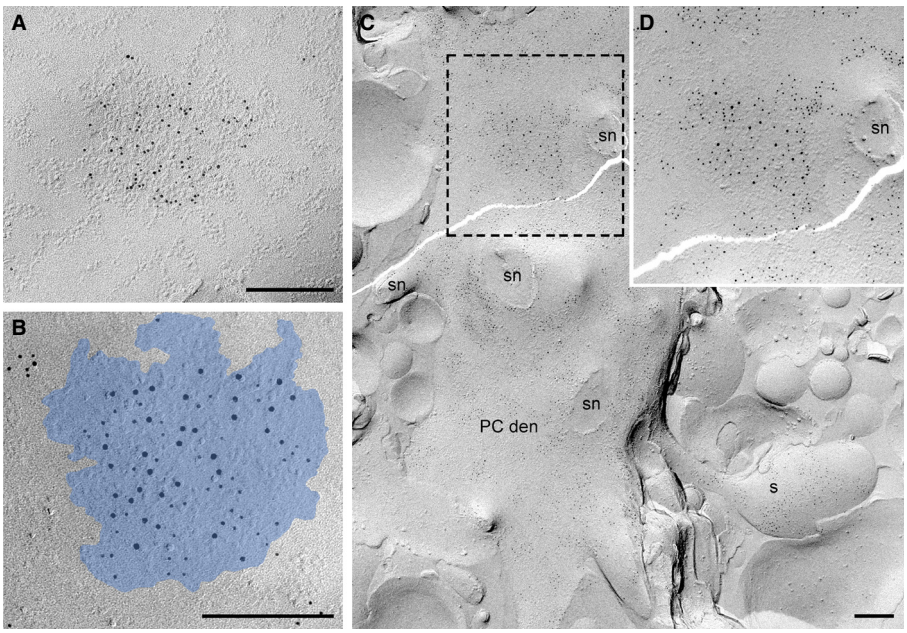

FIG. 3. Intrasynaptic localization of mGlu1α receptors in inhibitory synapses of the rat cerebellar cortex. (A) GABAergic synapses can be identified as IMP clusters immunolabelled for the $GABA_A$α1 subunit (6 nm gold) on the P-face of PC dendrites and somata. (B) Electron micrograph of a GABAergic synapse, characterized by the expression of $GABA_A$ receptors containing the α1 subunit (10 nm gold particles), on a PC dendrite (PSD revealed in blue) showing intrasynaptic labelling for mGlu1α receptors (5 nm gold particles). (C and D) A PC dendrite shows a widespread extrasynaptic labelling for mGlu1α receptors (5 nm). Note the strong labelling for mGlu1α present on the dendrite, spine and spine neck. (D) The inset shows the presence of mGlu1α receptors (5 nm gold particles) within the main body of a GABAergic synapse identified as the IMP cluster labelled for the $GABA_A$ α1 subunit (10 nm gold particles). PC den, PC dendrite; s, spine; sn, spine neck. Scale bars: 200 nm in A–C.

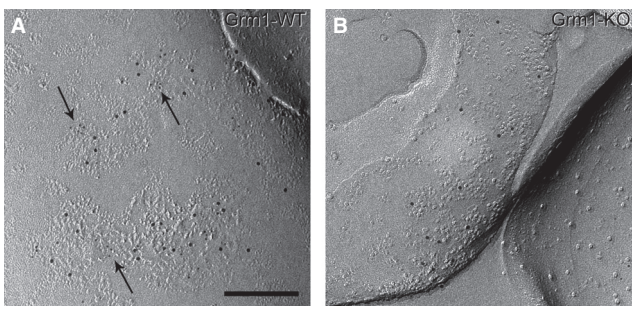

FIG. 4. Localization of mGlu1α receptor in the main body of inhibitory synapses in the mouse globus pallidus. (A) Arrows indicate 5 nm immunogold particles for mGlu1α receptor within an IMP cluster labelled for the $GABA_A$α1 subunit (10 nm). (B) No labelling for mGlu1α was detected in pallidal neurons of Grm1-KO mice. Grm1-KO, mGlu1-knock out; Grm1-WT, mGlu1-wild type. Scale bar: 200 nm.

Software, Inc.). The frequency of immunogold particles was measured in 60-nm-wide bins, keeping the edge of the synapse as 0. The distance data of gold particles from the synaptic edge obtained from different animals of the same species or treatment group were pooled. The density of immunogold particles detecting mGlu1α receptors in GABAergic synapses (total synaptic area analysed: 13.2 μm^2, measured from 131 synapses from three mice) and the extrasynaptic area (total synaptic area analysed: 241.0 μm^2) on the protoplasmic face (P-face) of mouse PCs was measured from digital images at 53 000× magnification with IMAGEJ (version 1.45S). Analysis of the frequency distributions of the gold particle distance between TAT-Homer1a-injected and TAT-Homer1aW24Y-injected mice was performed by means of the two-sample Kolmogorov–Smirnov test (SPSS Statistics software version 20, IBM). The density data for AMPA or Gluδ2 receptors were also pooled as there was no statistical difference between individual animals in the same group (Kruskal–Wallis test; AMPA, $P = 0.5$; Gluδ2, $P = 0.1$, control group). Data in text are given as mean ± SEM.

Results

Peri-synaptic enrichment of metabotropic glutamate receptors type 1 at glutamatergic parallel fibre–Purkinje cell synapses

Using the FRIL technique, we first re-examined the subcellular localization of the mGlu1α receptor isoform in the molecular layer of the rodent cerebellar cortex. Because the sequence specifying the mGlu1α receptor splice variant lies in the intracellular carboxy terminal tail, immunogold labelling was observed only on the P-face of replicas. In the cerebellar cortex, immunogold particles for mGlu1α receptors were observed throughout the PC soma, dendrites and spines including the spine neck. An apparent peri-synaptic enrichment of mGlu1α receptors was observed at PF–PC synapses (Fig. 1A). However, as the characteristic cluster of IMPs identifying glutamatergic synapses on the replica exoplasmic face cannot be seen on the P-face, we performed double-labelling experiments for mGlu1α and glutamate δ2 receptors. The glutamate δ2 receptor is an ionotropic receptor selectively present within the main body of PF–PC synapses; although it does not bind glutamate (Matsuda & Yuzaki, 2012) its gating is triggered by mGlu1 receptors (Ady *et al.*, 2014). These experiments confirmed the presence of mGlu1α receptors at the edge of the PSD of PF–PC synapses (Fig. 1B,C). The specificity of the immunolabelling was confirmed on replicas obtained from mGlu1-KO mice (Fig. 1D,E). It is noteworthy that some IMP clusters present on the P-face of PC dendrites were also found to be densely labelled for mGlu1α receptors.

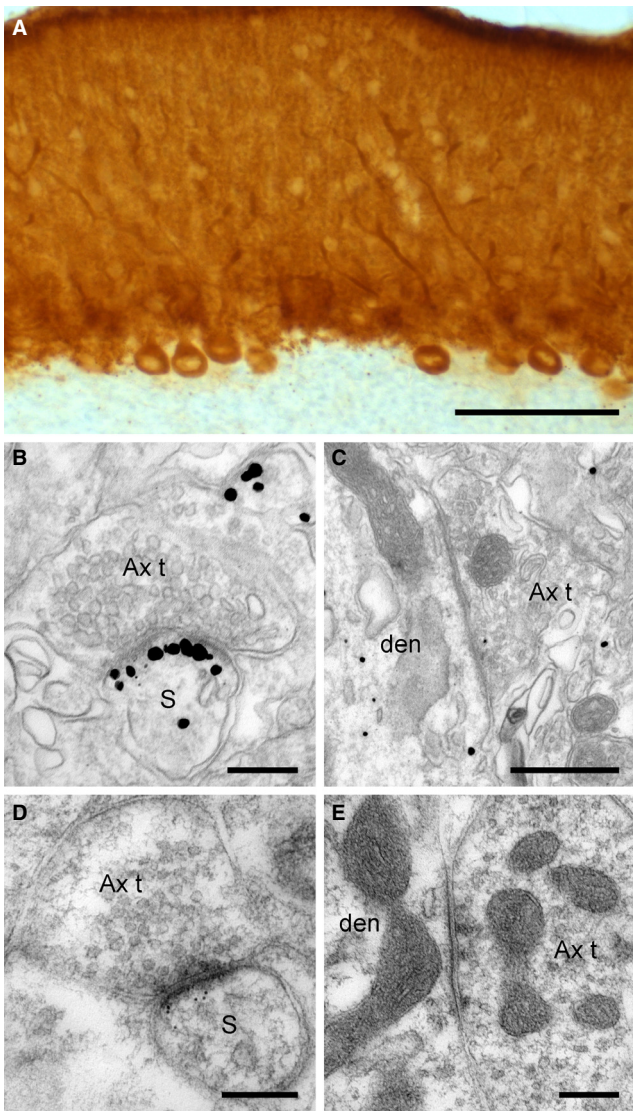

FIG. 5. Lack of expression of Homer3 at symmetric synapses of PCs. (A) Light micrograph showing Homer3 expression in somata and dendrites of PCs as revealed by 3-3′-diaminobenzidine/horseradish peroxidase staining. Pre-embedding (B and C) and post-embedding (D and E) were used to determine the subcellular localization of Homer3 in asymmetric and symmetric synapses in the cerebellar cortex. (B and D) Immunogold particles for Homer3 are abundantly detected in asymmetric synapses of the dendrites of PCs. (C and E) Homer3 labelling was not detected in symmetric synapses. Ax t, axon terminal; den, dendrite; s, spine. Scale bars: 100 μm in A; 200 nm in B, D and E; 500 nm in C.

The peri-synaptic enrichment of mGlu1 receptors at PF–PC synapses was further validated by double-labelling experiments for mGlu1 and δ2 receptors on both plasma membrane leaflets (Fig. 2A–D), using, for the detection of mGlu1 receptors on the exoplasmic face, an antibody raised against the extracellular N-terminus common to all mGlu1 receptor splice variants (Ferraguti *et al.*, 1998). To establish the relative density of mGlu1 receptors in relation to the synapse, the distance of gold particles from the nearest PSD boundary was measured. Our data clearly demonstrated a skewed distribution toward the extrasynaptic area with a preferential concentration of gold particles (~50%) in an arbitrarily chosen 60 nm segment spanning the PSD edge (Fig. 2E). Taken together, our findings obtained with the FRIL method demonstrated that the density of mGlu1 receptors was highest at the edge of PF–PC synapses, dropping markedly as a function of distance from the PSD boundary consistent with previous studies based on other techniques (Nusser *et al.*, 1994; Lujan *et al.*, 1997; Mateos *et al.*, 2000).

Intrasynaptic localization of metabotropic glutamate receptors type 1 at GABAergic synapses

Following the original observation of Somogyi and co-workers (Kasugai *et al.*, 2010) that, in replicas, GABAergic synapses can be visualized as clusters of IMPs on the P-face of hippocampal pyramidal cells, we also detected on the P-face of cerebellar PC dendrites IMP clusters strongly labelled for the $GABA_A$ receptor subunits α1 (Fig. 3A) and β3 or neuroligin 2 (data not shown). To establish whether mGlu1α receptor-labelled IMP clusters on PC dendrites correspond to GABAergic synapses, we carried out double-labelling experiments for the $GABA_A$ α1 subunit and mGlu1α receptor. Indeed, clear co-localization of the two molecules was detected within the main body of GABAergic synapses (Fig. 3B–D). To establish whether mGlu1 receptors are enriched in GABAergic synapses, we analysed the density of immunogold particles (5 nm) for mGlu1α receptors within GABAergic synapses (170.3 ± 13.8 gold particles/μm^2), identified by sequential labelling for $GABA_A$ α1 subunits, and in the nearby extrasynaptic areas (35.9 ± 3.5 gold particles/μm^2). GABAergic synapses showed a significantly higher density ($P < 0.0001$; Mann–Whitney test) with a ratio of 7.8 ± 0.8.

To further corroborate the intrasynaptic localization of mGlu1α receptors in GABAergic synapses, we examined, in replicas of the mouse globus pallidus, the co-existence between $GABA_A$ α1 subunits and mGlu1α receptors. Similar to what was observed in PC dendrites, IMP clusters onto the P-face of pallidal neuron dendrites also showed co-labelling for $GABA_A$ and mGlu1α receptors (Fig. 4). Taken together, these findings demonstrated a differential subsynaptic localization of mGlu1 receptors in neurochemically distinct synapses and validated previous pre-embedding studies (Hanson & Smith, 1999; Smith *et al.*, 2001).

Restricted localization of Homer3 to asymmetric synapses

The differential subsynaptic distribution of mGlu1 receptors between glutamatergic and GABAergic synapses raises the intriguing question of which molecular mechanisms are involved in the subcellular targeting of this receptor.

Homer proteins have been implicated in cross-linking group I mGlu receptors to inositol triphosphate receptors and phospholipase β4 (Brakeman *et al.*, 1997; Nakamura *et al.*, 2004). Several members of the Homer family have been identified (namely Homer1a, Homer1b-c, Homer2 and Homer3), which are characterized, with the exception of Homer1a, by a long coil-coiled carboxy terminal domain allowing multimerization (Xiao *et al.*, 1998, 2000). Subcellularly, it has been suggested that long Homers and mGlu1α receptors co-localize at the periphery of the PSD of glutamatergic synapses (Xiao *et al.*, 1998, 2000). Therefore, it can be hypothesized that long Homer proteins are involved in the specific peri-synaptic localization of mGlu1 receptor in glutamatergic synapses by restraining them from entering the post-synaptic specialization. The presence of mGlu1 receptors within GABAergic synapses would also be warranted by a lack of long Homer proteins in these synapses. In order to test this hypothesis, we used both pre-embedding and post-embedding techniques to reveal the subsynaptic distribution of the Homer3 protein, which is the most highly expressed long Homer isoform in the cerebellar cortex (Shiraishi *et al.*, 2004). Our results showed the enrichment of Homer3 immunoreactivity in PCs (Fig. 5A) and demonstrated that Homer3 was indeed exclusively present at

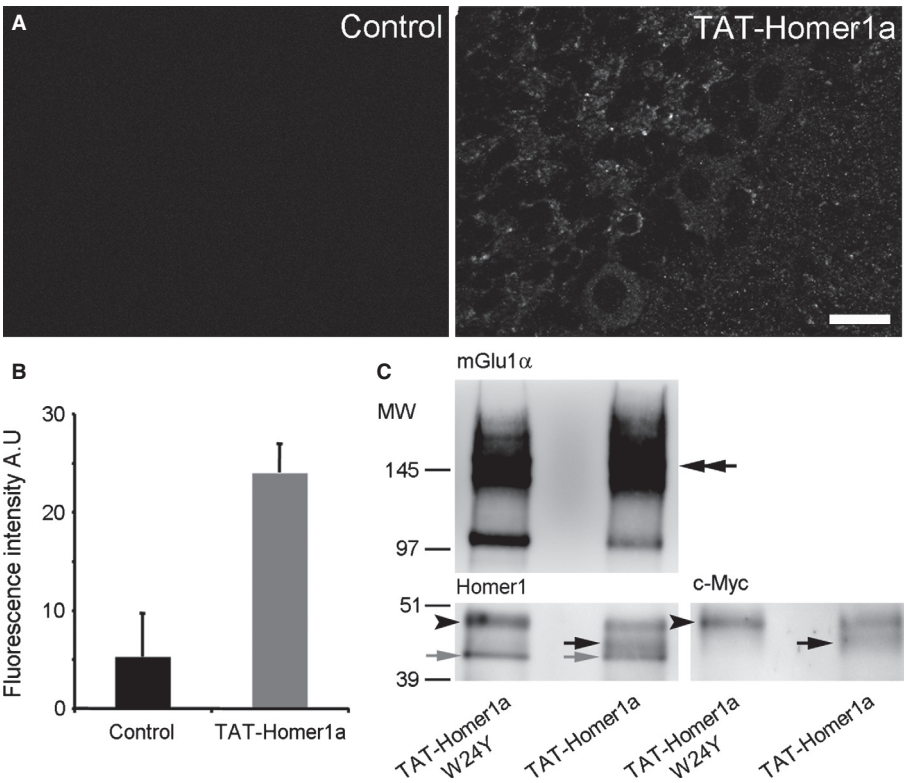

FIG. 6. Detection of TAT-Homer1a in the cerebellar cortex and interaction with mGlu1α receptors. (A) Intense anti-myc immunofluorescence revealing TAT-Homer1a can be observed in PCs, whereas no specific labelling was detected in the control saline-injected mice. (B) Fluorescence intensity was measured across the cerebellar cortex after intravenous injection of TAT-Homer1a or saline to assess the efficiency of cerebellar penetration of the constructs. (C) Co-immunoprecipitation of TAT-Homer1a with mGlu1α receptors from cerebellar detergent lysates of mice injected with TAT-Homer1a or TAT-Homer1aW24Y. The immunoprecipitated samples were subjected to immunoblot analysis in order to detect Myc-tagged TAT-Homer1a. The presence of an additional band (black arrow) above Homer1 (grey arrows, estimated molecular weight 43 kDa) in the TAT-Homer1a lane, but not in the TAT-Homer1aW24Y lane, should be noted. This band was also detected when the same polyvinylidene difluoride membrane was immunolabelled with anti-c-Myc antibodies. The double arrow indicates the band corresponding to the mGlu1α receptor. Arrowheads indicate light-chain IgGs used for immunoprecipitation. Scale bar: 20 μm in A. Data shown in B represent mean + SD. A.U., arbitrary units.

glutamatergic synapses (Fig. 5B,D). The absence of Homer3 labelling at GABAergic synapses (Fig. 5C,E) is thus in line with the hypothesis that long Homer proteins are involved in the peri-synaptic localization of mGlu1 receptors in glutamatergic synapses.

Homer1a-mediated disruption of long Homer complexes is not sufficient to alter metabotropic glutamate receptors type 1 peri-synaptic localization at parallel fibre–Purkinje cell synapses

Taking advantage of the dominant-negative property of Homer1a (Tu *et al.*, 1998), we investigated whether this short isoform could alter the distribution of mGlu1 receptors at PF–PC synapses by disrupting their binding with long Homers, hence allowing for higher mobility. Adult mice were infused through the tail vein with 8 mg/kg of either a cell-permeable TAT-conjugated form of Homer1a (TAT-Homer1a; $n = 6$) or a mutant version unable to bind to mGlu1 receptors (TAT-Homer1aW24Y; $n = 6$) (Moutin *et al.*, 2012). The two constructs contained a Myc tag, which was used to detect their penetration in PCs by immunofluorescence (Fig. 6A,B). To further confirm an interaction between mGlu1α receptors and TAT-Homer1a, a co-immunoprecipitation experiment using mGlu1α antibodies was carried out on cerebellar detergent lysates obtained from TAT-Homer1a-injected or TAT-Homer1aW24Y-injected mice. Co-immunoprecipitations with mGlu1α antibodies allowed the detection in TAT-Homer1a cerebellar eluates, but not in TAT-Homer1aW24Y, of a band revealed by both anti-Homer1 and c-Myc antibodies and consistent with the TAT-Homer1a protein (Fig. 6C).

To investigate the distribution of mGlu1 receptors in relation to the edge of glutamatergic synapses, mice were anaesthetized at 30 min after the tail vein injection of TAT-Homer1a or TAT-Homer1aW24Y, and their brains mildly fixed (1% paraformaldehyde) via transcardial perfusion. After slicing, specimens from the vermal portion of the cerebellar cortex were randomly selected from the molecular layer and processed for FRIL. Replicas were sequentially immunoreacted with N-terminal mGlu1 antibodies, visualized with secondary antibodies coupled with 5 nm gold particles, and pan-AMPA antibodies, and visualized with secondary antibodies coupled with 10 nm gold particles. The frequency distribution pattern of the distance of gold particles revealing mGlu1 receptors, as obtained from exoplasmic face replicas, from the synaptic edge did not differ (two-sample Kolmogorov–Smirnov test, $P = 0.34$) between TAT-Homer1a-injected and TAT-Homer1aW24Y-injected mice (number of particles analysed: TAT-Homer1aW24Y, $n = 1048$; TAT-Homer1a, $n = 1097$) (Fig. 7A,B). However, when the labelling density of AMPA receptors in the synaptic and extrasynaptic areas was analysed, a significant reduction in both domains could be detected in TAT-Homer1a-injected compared with TAT-Homer1aW24Y-injected mice (number of synapses analysed: TAT-Homer1aW24Y, 153; TAT-Homer1a, 179; Mann–Whitney test, synaptic $P = 0.00004$; extrasynaptic, $P = 0.027$) (Fig. 7C,D). These results showed the efficacy of the TAT-Homer1a injection

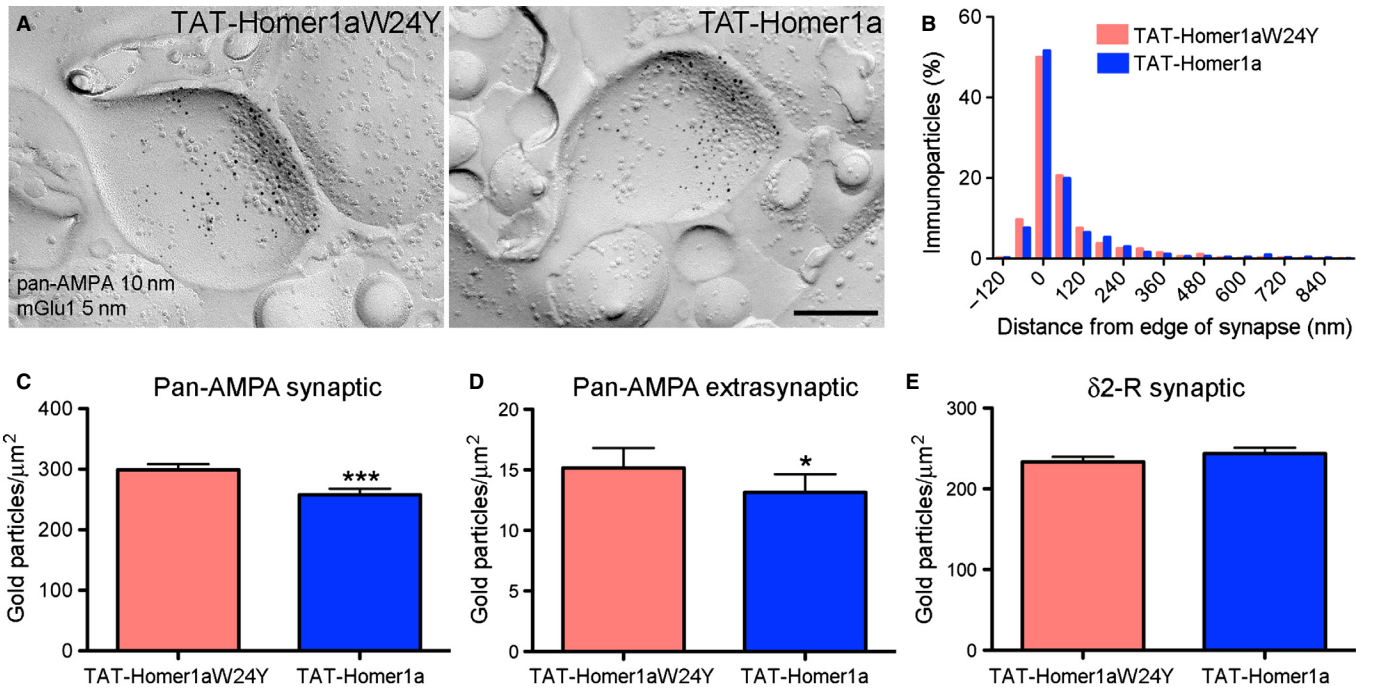

FIG. 7. Effect of TAT-Homer1a on mGlu1 receptor distribution pattern and density of AMPA and Gluδ2 receptors at PF–PC synapses. (A) Electron micrographs of PC spines (exoplasmic face) obtained from TAT-Homer1a-injected and TAT-Homer1aW24Y-injected mice, double labelled with 5 and 10 nm gold particles revealing mGlu1 and AMPA receptors, respectively. (B) Frequency distribution of 5 nm gold particles (mGlu1 receptor) relative to the PSD edge measured in 60-nm-wide bins. TAT-Homer1a did not influence the distribution pattern of the mGlu1 receptor (number of particles analysed: TAT-Homer1aW24Y, n = 1048; TAT-Homer1a, n = 1097; two-sample Kolmogorov–Smirnov test, P = 0.34). (C) The synaptic and (D) extrasynaptic density of AMPA receptors was measured in the same replicas, and found to be significantly reduced in both areas (number of synapses analysed: TAT-Homer1aW24Y, n = 153; TAT-Homer1a, n = 179; Mann–Whitney test, * $P < 0.05$, *** $P < 0.001$). (E) The synaptic density of gold particles for Gluδ2 receptors remained unchanged by TAT-Homer1a injection (number of synapses analysed: TAT-Homer1aW24Y, n = 163; TAT-Homer1a, n = 156; Mann–Whitney test, P = 0.167). Data in C–E represent mean + SEM. Scale bar in A: 200 nm.

despite the lack of influence on mGlu1 receptor distribution. Because of the known indirect interaction between glutamate δ2 and mGlu1 receptors (Kato *et al.*, 2012; Ohtani *et al.*, 2014), in another set of experiments we analysed, on replicas obtained from the same animals, the glutamate δ2 receptor density in PF–PC synapses. No difference in the synaptic density of glutamate 2 receptors was observed between the two groups of injected mice (n of synapses: TAT-Homer1aW24Y, 163; TAT-Homer1a, 156; Mann–Whitney test, P = 0.167) (Fig. 7E).

Discussion

Here, we provide the first unequivocal demonstration of the intrasynaptic localization of mGlu1 receptors in GABAergic synapses using the FRIL technique, and confirm their peri-junctional enrichment in glutamatergic synapses. Our findings highlight a fundamental difference in the subsynaptic localization of these receptors in neurochemically distinct types of synapse. Moreover, we show that the most abundant long Homer form in the cerebellar cortex, namely Homer3, is exclusively localized in asymmetric glutamatergic synapses consistent with its potential role in accumulating mGlu1 receptors peri-synaptically (Shiraishi-Yamaguchi & Furuichi, 2007). However, the dominant-negative TAT-Homer1a failed to significantly alter the distribution pattern of mGlu1 receptors with respect to the PSD. These findings suggest that the mGlu1–long Homer protein interaction is neither necessary nor sufficient for the peri-junctional accumulation of the receptor.

Homer proteins are known to interact with a proline-rich sequence present in the C-terminus of the mGlu1α receptor variant (Tu *et al.*, 1998), but absent in mGlu1β and mGlu1γ isoforms (Ferraguti *et al.*, 2008). All three splice variants are highly expressed in PCs (Berthele *et al.*, 1998; Ferraguti *et al.*, 2008) and the mGlu1β receptor shows a preferential peri-synaptic distribution similar to mGlu1α (Mateos *et al.*, 2000). So far no localization data are available for the mGlu1β variant, because no immunological tools have yet been developed. As Homer1a can disrupt only the interaction between mGlu1α and long Homer proteins, only a fraction of mGlu1 receptors might have been affected by the injection of TAT-Homer1a. This could have precluded the detection of a significant shift in mGlu1 receptor distribution near PF–PC synapses, in particular if mGlu1 splice variants do not heterodimerize (Remelli *et al.*, 2008), and given that we used a pan-mGlu1 antibody detecting all mGlu1 splice variants. However, we consider this possibility unlikely for a number of reasons. Firstly, the cumulative distribution of the distance of gold particles for mGlu1 receptors from the PSD edge between TAT-Homer1a-injected and TAT-Homer1aW24Y-injected mice was very similar. Secondly, in recent co-immunoprecipitation experiments performed with antibodies against mGlu1α followed by liquid chromatography mass spectrometry, we found unique peptides for both mGlu1α and mGlu1β receptor isoforms in the eluate, suggesting dimerization *in vivo* (Mansouri and Ferraguti, personal communication; see also Ohtani *et al.*, 2014). Thirdly, TAT-Homer1a also did not influence the synaptic density of δ2 receptors, which are known to be linked, although indirectly, to the C-terminal tail of mGlu1α receptors (Kato *et al.*, 2012; Ohtani *et al.*, 2014), probably through Shank (Uemura *et al.*, 2004).

Although we provide evidence that TAT-Homer1a penetrates in PCs, interacts with mGlu1α, and alters the AMPA receptor density

at the plasma membrane, our data do not rule out the possibility that TAT-Homer1a was unable to efficiently disrupt the interaction between endogenous Homer proteins and mGlu1 receptors, hence warranting further investigations. Definite proof for a role of Homer proteins in mGlu1 receptor subcellular targeting could be obtained, in our view, only by using genetically modified animals lacking all Homer genes, which, however, have not been developed so far.

Using the highly sensitive FRIL technique, we demonstrate a qualitatively and quantitatively matching mGlu1 subcellular distribution in rat and mouse PCs. Moreover, we show that mGlu1 receptors can be detected in both leaflets of the plasma membrane, suggesting no particular association with lipid subtypes. The planar view of large plasma membrane segments of PC spines, dendrites and somata offered by the FRIL technique allowed us to reveal the widespread extrasynaptic distribution of mGlu1 receptors. With respect to PF–PC synapses, it is noteworthy that we found a very similar frequency distribution of mGlu1 labelling tangential to the PSD as in previous reports, which used more conventional but less sensitive ultrastructural techniques (Baude *et al.*, 1993; Nusser *et al.*, 1994; Lujan *et al.*, 1997; Mateos *et al.*, 2000), when we adopted the same bin width (60 nm).

Previous studies suggested that mGlu1 receptors could reside in the main body of type II symmetric synapses on pallidal and nigral neurons (Hanson & Smith, 1999; Hubert *et al.*, 2001). Our findings extend this work and provide conclusive evidence for the intrasynaptic localization of mGlu1 receptors in GABAergic synapses onto PCs as well as on pallidal neurons. The direct presence of mGlu1 receptors in GABAergic synapses raises important questions concerning their functional role as well as about the source of glutamate needed for their activation.

Several forms of plasticity of inhibitory transmission have been reported to occur in cerebellar PCs, which include RP and DSI (Kano *et al.*, 1992; Galante & Diana, 2004). Both DSI and RP were shown to require activation of mGlu1 receptors (Galante & Diana, 2004; Sugiyama *et al.*, 2008). Although depolarization-induced elevations of intracellular Ca^{2+} can lead to both depolarization-induced suppression of excitation and DSI, the induction of DSI by mGlu1 receptors was independent of post-synaptic Ca^{2+} increases and involved endocannabinoids retrogradely acting on pre-synaptic type 1 cannabinoid receptors, which in turn inhibit neurotransmitter release (Galante & Diana, 2004). The current hypothesis posits that activation of mGlu1 receptors by glutamate released from PFs would allow the diffusion of endocannabinoids from their sites of release at glutamatergic synapses to reach interneuron pre-synaptic terminals, hence determining DSI. Our findings may provide an alternative interpretation. Brief depolarization of PCs triggers dendritic release of glutamate in the extracellular space (Duguid *et al.*, 2007; Shin *et al.*, 2008), which is more likely to diffuse to interneuron–PC synapses than to PF–PC or climbing fibre–PC synapses because of the high concentration of glutamate transporters surrounding these latter synapses (Chaudhry *et al.*, 1995). Glutamate could then stimulate mGlu1 receptors in GABAergic synapses and induce the consequent local production of endocannabinoids.

An indirect effect of mGlu1 receptor activation has also been postulated for the regulation of RP, although independent of the Gαq/phospholipase Cβ4 pathway typical of mGlu1 receptors present at glutamatergic synapses (Sugiyama *et al.*, 2008). The induction of RP by mGlu1 receptors was shown to be mediated through the Gαs/protein kinase A/dopamine- and cAMP-regulated phosphoprotein-32 signalling pathway (Sugiyama *et al.*, 2008). The direct identification of mGlu1 receptors in GABAergic synapses suggests a novel scenario for their contribution to RP, and provides a plausible option for the formation by these receptors of a different protein complex as well as the coupling to a distinct intracellular signalling cascade from glutamatergic synapses. The recent observation that mGlu1 receptors in the cerebellar cortex participate in the vestibulo-ocular reflex motor learning (Titley *et al.*, 2010) may be explained through a direct regulation of RP (Tanaka *et al.*, 2013) at GABAergic synapses rather than an influence on PF–PC long-term depression of excitatory transmission (Titley *et al.*, 2010), or alternatively a combination of these two effects. At this point, our interpretation is purely speculative; further studies are needed to clarify this issue.

In conclusion, taking advantage of the FRIL technique, we unequivocally demonstrate the localization of mGlu1 receptors within the PSD of GABAergic synapses, confirm their preferential peri-junctional accumulation at glutamatergic synapses and reveal a widespread extrasynaptic distribution in the somato-dendritic compartment of PCs. Moreover, we propose that disruption of the interaction between mGlu1 receptors and long Homer proteins, apparently restricted to asymmetric synapses, does not significantly alter the distribution pattern of the mGlu1 receptor at PF–PC synapses, suggesting that other scaffolding proteins are involved in their peri-synaptic confinement. The identification of interactors that regulate the subsynaptic localization of the mGlu1 receptor at neurochemically distinct synapses may offer new insight into its trafficking, intracellular signalling and function.

Acknowledgements

The authors thank S. Schönherr for excellent technical support and Dr Furuichi for kindly providing anti-Homer3 antibodies. This work was supported by the Austrian Science Fund (FWF) (project W012060-10 to F.F.), The Japan Society for the Promotion of Science (JSPS) (to R.S.) and Agence Nationale de la Recherche (ANR-11-BSV4-018-03, DELTAPLAN), Région Languedoc-Roussillon (Chercheur d'Avenir) (to J.P.). We declare that none of the authors have any conflict of interest.

Abbreviations

DSI, depolarization-induced suppression of inhibition; FRIL, freeze-fracture replica immunogold labelling; IMP, intramembrane particle; KO, knockout; mGlu1, metabotropic glutamate receptor type 1; PB, phosphate buffer; PBS, phosphate-buffered saline; PC, Purkinje cell; PF, parallel fibre; P-face, protoplasmic face; PSD, post-synaptic density; RP, rebound potentiation; RT, room temperature; TBS, Tris-buffered saline; TBS-T, Tris-buffered saline containing 0.1% Triton X-100.

References

Ady, V., Perroy, J., Tricoire, L., Piochon, C., Dadak, S., Chen, X., Dusart, I., Fagni, L., Lambolez, B. & Levenes, C. (2014) Type 1 metabotropic glutamate receptors (mGlu1) trigger the gating of GluD2 delta glutamate receptors. *EMBO Rep.*, **15**, 103–109.

Aiba, A., Kano, M., Chen, C., Stanton, M.E., Fox, G.D., Herrup, K., Zwingman, T.A. & Tonegawa, S. (1994) Deficient cerebellar long-term depression and impaired motor learning in mGluR1 mutant mice. *Cell*, **79**, 377–388.

Baude, A., Nusser, Z., Roberts, J.D., Mulvihill, E., McIlhinney, R.A. & Somogyi, P. (1993) The metabotropic glutamate receptor (mGluR1 alpha) is concentrated at perisynaptic membrane of neuronal subpopulations as detected by immunogold reaction. *Neuron*, **11**, 771–787.

Berthele, A., Laurie, D.J., Platzer, S., Zieglgänsberger, W., Tölle, T.R. & Sommer, B. (1998) Differential expression of rat and human type I metabotropic glutamate receptor splice variant messenger RNAs. *Neuroscience*, **85**, 733–749.

Boyden, E.S., Katoh, A. & Raymond, J.L. (2004) Cerebellum-dependent learning: the role of multiple plasticity mechanisms. *Annu. Rev. Neurosci.*, **27**, 581–609.

Brakeman, P.R., Lanahan, A.A., O'Brien, R., Roche, K., Barnes, C.A., Huganir, R.L. & Worley, P.F. (1997) Homer: a protein that selectively binds metabotropic glutamate receptors. *Nature*, **386**, 284–288.

Chaudhry, F.A., Lehre, K.P., van Lookeren Campagne, M., Ottersen, O.P., Danbolt, N.C. & Storm-Mathisen, J. (1995) Glutamate transporters in glial plasma membranes: highly differentiated localizations revealed by quantitative ultrastructural immunocytochemistry. *Neuron*, **15**, 711–720.

Conquet, F., Bashir, Z.I., Davies, C.H., Daniel, H., Ferraguti, F., Bordi, F., Franz-Bacon, K., Reggiani, A., Matarese, V., Conde, F., Collingridge, G.L. & Crepel, F. (1994) Motor deficit and impairment of synaptic plasticity in mice lacking mGluR1. *Nature*, **372**, 237–243.

Duguid, I.C., Pankratov, Y., Moss, G.W. & Smart, T.G. (2007) Somatodendritic release of glutamate regulates synaptic inhibition in cerebellar Purkinje cells via autocrine mGluR1 activation. *J. Neurosci.*, **27**, 12464–12474.

Dzubay, J.A. & Otis, T.S. (2002) Climbing fiber activation of metabotropic glutamate receptors on cerebellar Purkinje neurons. *Neuron*, **36**, 1159–1167.

Ferraguti, F., Conquet, F., Corti, C., Grandes, P., Kuhn, R. & Knopfel, T. (1998) Immunohistochemical localization of the mGluR1 beta metabotropic glutamate receptor in the adult rodent forebrain: evidence for a differential distribution of mGluR1 splice variants. *J. Comp. Neurol.*, **400**, 391–407.

Ferraguti, F., Crepaldi, L. & Nicoletti, F. (2008) Metabotropic glutamate 1 receptor: current concepts and perspectives. *Pharmacol. Rev.*, **60**, 536–581.

Galante, M. & Diana, M.A. (2004) Group I metabotropic glutamate receptors inhibit GABA release at interneuron-Purkinje cell synapses through endocannabinoid production. *J. Neurosci.*, **24**, 4865–4874.

Hanson, J.E. & Smith, Y. (1999) Group I metabotropic glutamate receptors at GABAergic synapses in monkeys. *J. Neurosci.*, **19**, 6488–6496.

Hubert, G.W., Paquet, M. & Smith, Y. (2001) Differential subcellular localization of mGluR1a and mGluR5 in the rat and monkey substantia nigra. *J. Neurosci.*, **21**, 1838–1847.

Ito, M. (2001) Cerebellar long-term depression: characterization, signal transduction, and functional roles. *Physiol. Rev.*, **81**, 1143–1195.

Ito, M. (2006) Cerebellar circuitry as a neuronal machine. *Prog. Neurobiol.*, **78**, 272–303.

Kano, M., Rexhausen, U., Dreessen, J. & Konnerth, A. (1992) Synaptic excitation produces a long-lasting rebound potentiation of inhibitory synaptic signals in cerebellar Purkinje cells. *Nature*, **356**, 601–604.

Kano, M., Hashimoto, K. & Tabata, T. (2008) Type-1 metabotropic glutamate receptor in cerebellar Purkinje cells: a key molecule responsible for long-term depression, endocannabinoid signalling and synapse elimination. *Philos. T. Roy. Soc. B.*, **363**, 2173–2186.

Kasugai, Y., Swinny, J.D., Roberts, J.D., Dalezios, Y., Fukazawa, Y., Sieghart, W., Shigemoto, R. & Somogyi, P. (2010) Quantitative localisation of synaptic and extrasynaptic GABA-A receptor subunits on hippocampal pyramidal cells by freeze-fracture replica immunolabelling. *Eur. J. Neurosci.*, **32**, 1868–1888.

Kato, A.S., Knierman, M.D., Siuda, E.R., Isaac, J.T., Nisenbaum, E.S. & Bredt, D.S. (2012) Glutamate receptor δ2 associates with metabotropic glutamate receptor 1 (mGluR1), protein kinase Cγ, and canonical transient receptor potential 3 and regulates mGluR1-mediated synaptic transmission in cerebellar Purkinje neurons. *J. Neurosci.*, **32**, 15296–15308.

Kaufmann, W.A., Ferraguti, F., Fukazawa, Y., Kasugai, Y., Shigemoto, R., Laake, P., Sexton, J.A., Ruth, P., Wietzorrek, G., Knaus, H.G., Storm, J.F. & Ottersen, O.P. (2009) Large-conductance calcium-activated potassium channels in purkinje cell plasma membranes are clustered at sites of hypolemmal microdomains. *J Comp. Neurol.*, **515**, 215–230.

Lujan, R., Roberts, J.D., Shigemoto, R., Ohishi, H. & Somogyi, P. (1997) Differential plasma membrane distribution of metabotropic glutamate receptors mGluR1 alpha, mGluR2 and mGluR5, relative to neurotransmitter release sites. *J. Chem. Neuroanat.*, **13**, 219–241.

Maejima, T., Hashimoto, K., Yoshida, T., Aiba, A. & Kano, M. (2001) Presynaptic inhibition caused by retrograde signal from metabotropic glutamate to cannabinoid receptors. *Neuron*, **31**, 463–475.

Masugi-Tokita, M. & Shigemoto, R. (2007) High-resolution quantitative visualization of glutamate and GABA receptors at central synapses. *Curr. Opin. Neurobiol.*, **17**, 387–393.

Mateos, J.M., Benitez, R., Elezgarai, I., Azkue, J.J., Lazaro, E., Osorio, A., Bilbao, A., Donate, F., Sarria, R., Conquet, F., Ferraguti, F., Kuhn, R., Knopfel, T. & Grandes, P. (2000) Immunolocalization of the mGluR1b splice variant of the metabotropic glutamate receptor 1 at parallel fiber-Purkinje cell synapses in the rat cerebellar cortex. *J. Neurochem.*, **74**, 1301–1309.

Matsuda, K. & Yuzaki, M. (2012) Cbln1 and the δ2 glutamate receptor - an orphan ligand and an orphan receptor find their partners. *Cerebellum*, **11**, 78–84.

Moutin, E., Raynaud, F., Roger, J., Pellegrino, E., Homburger, V., Bertaso, F., Ollendorff, V., Bockaert, J., Fagni, L. & Perroy, J. (2012) Dynamic remodeling of scaffold interactions in dendritic spines controls synaptic excitability. *J. Cell Biol.*, **198**, 251–263.

Nakamura, M., Sato, K., Fukaya, M., Araishi, K., Aiba, A., Kano, M. & Watanabe, M. (2004) Signaling complex formation of phospholipase Cbeta4 with metabotropic glutamate receptor type 1alpha and 1,4,5-trisphosphate receptor at the perisynapse and endoplasmic reticulum in the mouse brain. *Eur. J. Neurosci.*, **20**, 2929–2944.

Nusser, Z., Mulvihill, E., Streit, P. & Somogyi, P. (1994) Subsynaptic segregation of metabotropic and ionotropic glutamate receptors as revealed by immunogold localization. *Neuroscience*, **61**, 421–427.

Ohtani, Y., Miyata, M., Hashimoto, K., Tabata, T., Kishimoto, Y., Fukaya, M., Kase, D., Kassai, H., Nakao, K., Hirata, T., Watanabe, M., Kano, M. & Aiba, A. (2014) The synaptic targeting of mGluR1 by its carboxyl-terminal domain is crucial for cerebellar function. *J. Neurosci.*, **34**, 2702–2712.

Perroy, J., Raynaud, F., Homburger, V., Rousset, M.C., Telley, L., Bockaert, J. & Fagni, L. (2008) Direct interaction enables cross-talk between ionotropic and group-I metabotropic glutamate receptors. *J. Biol. Chem.*, **283**, 6799–6805.

Raymond, J.L., Lisberger, S.G. & Mauk, M.D. (1996) The cerebellum: a neuronal learning machine? *Science*, **272**, 1126–1131.

Remelli, R., Robbins, M.J. & McIlhinney, R.A. (2008) The C-terminus of the metabotropic glutamate receptor 1b regulates dimerization of the receptor. *J. Neurochem.*, **104**, 1020–1031.

Shigemoto, R., Abe, T., Nomura, S., Nakanishi, S. & Hirano, T. (1994) Antibodies inactivating mGluR1 metabotropic glutamate receptor block long-term depression in cultured Purkinje cells. *Neuron*, **12**, 1245–1255.

Shin, J.H., Kim, Y.S. & Linden, D.J. (2008) Dendritic glutamate release produces autocrine activation of mGluR1 in cerebellar Purkinje cells. *Proc. Natl. Acad. Sci. USA*, **105**, 746–750.

Shiraishi, Y., Mizutani, A., Yuasa, S., Mikoshiba, K. & Furuichi, T. (2004) Differential expression of Homer family proteins in the developing mouse brain. *J. Comp. Neurol.*, **473**, 582–599.

Shiraishi-Yamaguchi, Y. & Furuichi, T. (2007) The Homer family proteins. *Genome Biol.*, **8**, 206.

Smith, Y., Charara, A., Paquet, M., Kieval, J.Z., Pare, J.F., Hanson, J.E., Hubert, G.W., Kuwajima, M. & Levey, A.I. (2001) Ionotropic and metabotropic GABA and glutamate receptors in primate basal ganglia. *J. Chem. Neuroanat.*, **22**, 13–42.

Sreepathi, H.K. & Ferraguti, F. (2012) Subpopulations of neurokinin 1 receptor-expressing neurons in the rat lateral amygdala display a differential pattern of innervation from distinct glutamatergic afferents. *Neuroscience*, **203**, 59–77.

Sugiyama, Y., Kawaguchi, S. & Hirano, T. (2008) mGluR1-mediated facilitation of long-term potentiation at inhibitory synapses on a cerebellar Purkinje neuron. *Eur. J. Neurosci.*, **27**, 884–896.

Tanaka, S., Kawaguchi, S.Y., Shioi, G. & Hirano, T. (2013) Long-term potentiation of inhibitory synaptic transmission onto cerebellar Purkinje neurons contributes to adaptation of vestibulo-ocular reflex. *J. Neurosci.*, **33**, 17209–17220.

Titley, H.K., Heskin-Sweezie, R. & Broussard, D.M. (2010) The bidirectionality of motor learning in the vestibulo-ocular reflex is a function of cerebellar mGluR1 receptors. *J. Neurophysiol.*, **104**, 3657–3666.

Tu, J.C., Xiao, B., Yuan, J.P., Lanahan, A.A., Leoffert, K., Li, M., Linden, D.J. & Worley, P.F. (1998) Homer binds a novel proline-rich motif and links group 1 metabotropic glutamate receptors with IP3 receptors. *Neuron*, **21**, 717–726.

Uemura, T., Mori, H. & Mishina, M. (2004) Direct interaction of GluR 2 with Shank scaffold proteins in cerebellar Purkinje cells. *Mol. Cell. Neurosci.*, **26**, 330–341.

Wang, W., Nakadate, K., Masugi-Tokita, M., Shutoh, F., Aziz, W., Tarusawa, E., Lorincz, A., Molnár, E., Kesaf, S., Li, Y.Q., Fukazawa, Y., Nagao, S. & Shigemoto, R. (2014) Distinct cerebellar engrams in short-term and long-term motor learning. *Proc. Natl. Acad. Sci. USA*, **111**, 188–193.

Xiao, B., Tu, J.C., Petralia, R.S., Yuan, J.P., Doan, A., Breder, C.D., Ruggiero, A., Lanahan, A.A., Wenthold, R.J. & Worley, P.F. (1998) Homer regulates the association of group 1 metabotropic glutamate receptors with multivalent complexes of homer-related, synaptic proteins. *Neuron*, **21**, 707–716.

Xiao, B., Tu, J.C. & Worley, P.F. (2000) Homer: a link between neural activity and glutamate receptor function. *Curr. Opin. Neurobiol.*, **10**, 370–374.